

DETERMINATION OF TENSION FOR POLYAMIDE AND BASALT MULTIFILAMENT YARNS WHILE WEAVING INDUSTRIAL FABRICS

Volodymyr Shcherban¹, Oksana Kolysko¹, Gennadiy Melnyk¹, Marijna Sholudko¹,
Yuriy Shcherban², Ganna Shchutska² and Nikita Kolva¹

¹Kyiv National University of Technologies and Design, Nemirovicha-Danchenko str., 2, 01011 Kyiv, Ukraine

²Department of Light Industry Technologies State Higher Educational Establishment «Kyiv College of Light Industry»
Ivana Kudri str., 29, 01601 Kyiv, Ukraine
melnik2000@ukr.net

Abstract: Resulting from researches aimed at determination of tension for polyamide and basalt multifilament yarns while interacting with guides and operative parts of looms in the process of industrial fabrics formation, yarn tension increase according to filling areas has been found out by applying different geometrical dimensions and due to friction forces in the contact area. It has been proved that tension degree of polyamide and basalt multifilament yarns before industrial fabrics formation area is affected by the following parameters: tension prior going to guide surface, radius of guide surface curve, contact angle with yarns of guide surface, as well as mechanical, physical and structural properties of polyamide and basalt multifilament yarns. Thus, allowing to determine tension of the polyamide and basalt multifilament yarns before industrial fabrics formation area yet at the initial stages of computer aided manufacturing taking into account loom parameters, shape of yarn filling line, mechanical, physical and structural properties of yarns and industrial fabrics. This article represents the experimental research of interaction between polyamide and basalt multifilament yarns having cylindrical surfaces, imitating separating rod of yarn break detector, as well as heddle eye for automatic looms. Based on experimental researches for polyamide and basalt multifilament yarns the regression dependencies between tension degree after guide and guide's curve radius, yarn tension before guide and nominal value of contact angle has been obtained. Consistent application of the data of regression dependencies allows to determine tension of polyamide and basalt multifilament yarns before the industrial fabrics formation area. Analysis of regression dependencies helped to find out values of technological parameters, in case when polyamide and basalt multifilament yarns tension before the industrial fabrics formation areas shall have minimum value. The foregoing will make it possible to apply minimum tension of polyamide and basalt multifilament yarns for their processing at looms. Thus, it leads to reduction in yarn breakages, more efficient performance of production equipment due to reduced downtime, as well as enhanced quality of industrial fabrics. Therefore, we can argue that offered technological solutions are practically attractive. Consequently, it is reasonable to speak of possible guided management as for process of change in tension of polyamide and basalt multifilament yarns when forming industrial fabrics using looms by means of selecting geometrical dimensions for guides.

Keywords: tension, polyamide and basalt multifilament yarn, radius of guide surface curve, contact angle.

1 INTRODUCTION

Technical fabrics made of polyamide and basalt multifilament yarns are widely used for various purposes in different industry fields. Their unique mechanical and physical properties fully explain the previous statement. The technological process of manufacturing of industrial fabrics from polyamide and basalt multifilament yarns requires for improvement enhanced technological efforts based on minimized warp yarn tension in the fabric weaving area. The value of warp yarn tension, before they enter industrial fabric weaving area, determines density of weaving process, as well as compactness of fabric structure [1-3]. Tension of polyamide and basalt multifilament warp yarns,

before they enter industrial fabric weaving area, comprises threading tension and additional tension that is driven by friction force between warp yarns and surfaces of a loom guides and operative parts having cylindrical and near-cylindrical form [4].

Progress density of technological process can be measured by determining value of yarn tension (during spun yarn winding) in operative areas of the technological machine [5, 6], loom [7, 8], or knitting machines [2, 9]. Main characteristic property of the most technological processes in textile industry is interaction between yarns and guides and operative parts, when guide's surface curvature radius in the area of contact is comparable to the yarn diameter [10, 11].

Polyamide and basalt multifilament yarns manufacturing process simulation on a loom involves research of interaction process between warp yarns with cylindrical surfaces imitating ones of back rest, of separating rod of yarn break detector, and of heddle eyes of heald frame for automatic looms [8]. Increase in yarn tension depends on friction forces in the area of contact with guides. The value of friction forces changes with regard to yarns material and guide, their geometrical dimensions ratio (i.e., of yarn diameter radius to guide's curvature radius in the contact area), actual contact angle between a yarn and a guide and radial contact angle between a yarn and a guide surface, mechanical, physical and structural properties of polyamide and basalt multifilament yarns, their tension before guide. When a yarn passes all guides consecutively, from the guide in the threading area and up to the guide in the fabric weaving area, it leads to step-type increase in tension. The value of output tension after previous guide will be the threading parameter for the following guide, thus allowing for use of recursion to determine tension of a yarn before it enters industrial fabric weaving area [12, 13].

Experimental research conducted to determine tension of polyamide and basalt multifilament yarns after guide surface requires designing specific strain-gauge unit. In a proactive planning of the experiment, it is necessary to consider the following: direction of relative shifting of friction surface [14], yarn sliding speed or guide surface movement speed [15, 16], and radius of guide surface curve [17, 18]. The paper [19] emphasizes necessity to consider that spinning of polyamide multifilament yarns affects their bending rigidity. Bending rigidity is significantly affecting the value of actual contact angle between a yarn and guide surface. This has been verified during the research of interaction conditions between polyamide multifilament yarn and guide surface and represented in the paper [10, 11] afterwards.

The papers show results of experimental determining of yarn tension with the use of specific units [8-12]. To increase accuracy of measured polyamide and basalt multifilament yarn tension and possibility of ensuring the metrological self-verification it is better to rely on the method of redundant measurements, which ensures that results of measurements are independent from conversion function parameters, and their deviations are independent from reference values [21, 22]. Design of the experimental unit measures accuracy of the obtained results while determining yarn tension. The paper [17] shows the scheme, which helps to determine yarn tension, and includes cylinders with long radius as guides. As its deficiency, it is important to consider inability to simulate actual conditions of interaction between yarn and guide and operative parts of looms and

knitting machines. Experimental unit with revolving cylinder has the same deficiency [18]. Papers [2, 8-10, 15, 20] represent tension determinations for a variety of cylindrical guide surfaces.

2 EXPERIMENT

The paper had the four variants of research planned. For variant 1A the polyamide multifilament yarn 29x6 tex was chosen. For variant 2B the polyamide multifilament yarn 93.5x3 tex was chosen. For variant 3C the basalt multifilament yarn 250 tex was chosen. For variant 4D the basalt multifilament yarn 330 tex was chosen. USB Digital microscope Sigeta (Figure 1a) was used to determine dimensions of yarns diameters. The number of experiments to determine diameter for each multifilament yarn depended on value of confidence factor ($\alpha = 0.95$) and value of confidence error for the average result $\varepsilon(\bar{x}) = 0.1\bar{x}$, where \bar{x} is an arithmetic mean value of multifilament yarns diameter. Having reference value of confidence factor, values of confidence error and number of measurements were determined with the help of calculated Student criterion values. Obtained value shall be greater than the one in the table. Figure 1b shows the polyamide multifilament yarn. Figure 1c shows the basalt multifilament yarn.

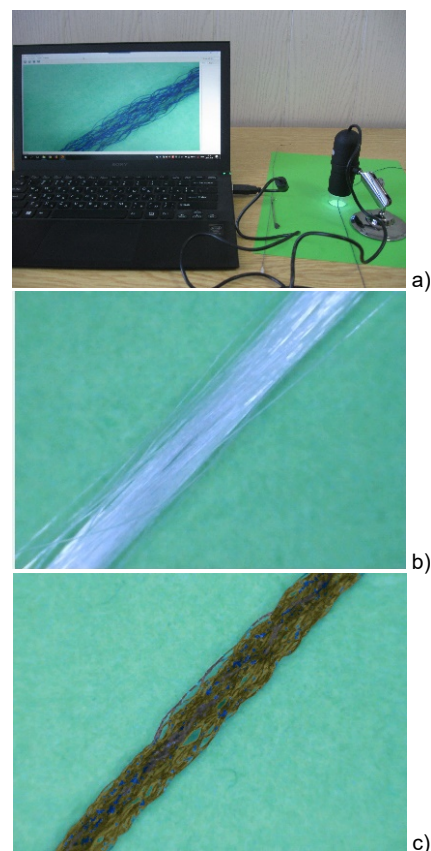


Figure 1 Determining dimensions of yarns diameters: a) device determining the diameter; b) polyamide multifilament yarn; c) basalt multifilament yarn

Polyamide multifilament yarns 29x6 tex (variant 1A) were used as warp in manufacture of multilayer industrial fabric MTF – 5, which is intended for laying yard-coated pipes. This fabric is manufactured with warp setting of 120 ends per 100 mm and weft setting of 140 ends per 100 mm. Such fabric comprises five layers (Figure 2a), outer layers were formed by plain weave with threading being 400 mm wide [13]. Polyamide multifilament yarns 93.5x3 tex (variant 2B) were used as warp to manufacture multilayer industrial fabric MTF – 7 (Figure 2b), which is intended for laying yard-coated pipes as a bearing in transporting equipment. This fabric is manufactured with warp setting of 110 ends per 100 mm and weft setting of 120 ends per 100 mm. This fabric has five layers and weaving width of 600 mm.

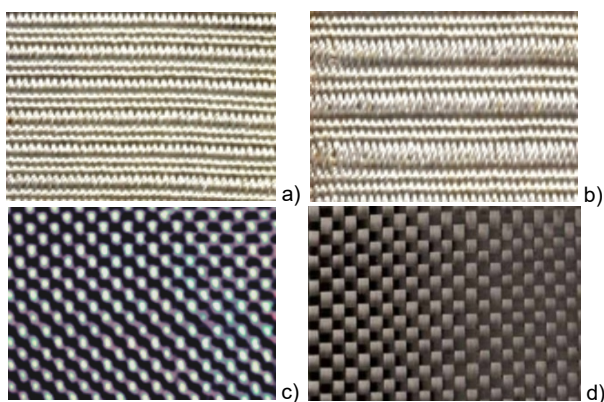


Figure 2 Industrial fabrics of polyamide and basalt multifilament yarns: a) multilayer industrial fabric MTF – 5; b) multilayer industrial fabric MTF – 7; c) basalt fabric of plain weave; d) fire-resistant basalt fabric of plain weave

Basalt multifilament yarns 250 tex (variant 3C) were used as warp to manufacture basalt fabric of plain weave (Figure 2c), which is incorporated into power units and used for thermal insulation of pipelines. This fabric is manufactured with warp setting of 80 ends per 100 mm and weft setting of 60 ends per 100 mm. Basalt multifilament yarns 330 tex (variant 4D) were used as a warp to manufacture fire-resistant basalt fabric of plain weave (Figure 2d). This fabric is manufactured with warp setting

of 90 ends per 100 mm and with weft setting 70 ends per 100 mm.

Tension of warp yarns (before they enter weaving area) is a value determining density of weaving process. Tension of polyamide and basalt warp yarns (before they enter fabric weaving area) comprises threading tension and additional tension that is driven by friction force between warp yarns and surfaces of a loom guides and operative parts having cylindrical and near-cylindrical form. Warp yarn threading line on a loom is made-up of three areas: I area – between the beam and dropper separating mechanism; II area – between back rest and heald frames; III area – between dropper separating mechanism and fell of the fabric. Warp yarns interact with back rest in I area. In II area a contact between yarns and a dropper separating unit occurs. And warp yarns contact heddle eye of heald frame in III area.

For variants 1A, 2B, 3C and 4D the paper provides a plan and implementation of the second-order orthogonal matrix for three factors to determine combined influence of slack side tension of warp yarn P_0 , cylindrical guide radius R , and nominal value of contact angle φ_p to tight side tension of warp yarn P . Overall form of regression equation is as follows:

$$P = b_0 + b_1x_1 + b_2x_2 + b_3x_3 + b_{12}x_1x_2 + b_{13}x_1x_3 + b_{23}x_2x_3 + b_{11}x_1^2 + b_{22}x_2^2 + b_{33}x_3^2 \quad (1)$$

Range of factors variations in equation (1) was determined under polyamide and basalt multifilament yarns actual weaving conditions on looms.

Factor x_1 is a value of threading tension of polyamide and basalt multifilament yarns in the I area before the back rest. Variant 1A is for polyamide multifilament yarn 29x6 tex and the value ranged within following limits $P_{011} = 25-35$ cN. Variant 2B is for polyamide multifilament yarn 93.5x3 tex and the value ranged within following limits $P_{012} = 40-55$ cN. Variant 3C for basalt multifilament yarn 250 tex and the value ranged within following limits $P_{013} = 20-30$ cN. Variant 4D for basalt multifilament yarn 330 tex and the value ranged within following limits $P_{014} = 20-30$ cN.

Table 1 The scheme of experimental researches

Fabric	Properties	Determining tension in an area [cN]		
<i>Variant 1A</i> Multilayer technical fabric MTF – 5	Warp setting of 120 ends per 100 mm; Weft setting of 140 ends per 100 mm	I area between the beam and the dropper separating mechanism	II area between the back- rest and heald frames	III area between the dropper separating mechanism and fell of the fabric
<i>Variant 2B</i> Multilayer technical fabric MTF – 7	Warp setting of 110 ends per 100 mm; Weft setting of 120 ends per 100 mm			
<i>Variant 3C</i> Basalt fabric of plain weave	Warp setting of 80 ends per 100 mm; Weft setting of 60 ends per 100 mm			
<i>Variant 4D</i> Fire-resistant basalt fabric of plain weave	Warp setting of 90 ends per 100 mm; Weft setting of 70 ends per 100 mm			

Factor x_2 is a cylinder (back rest) radius in I area that ranged within following limits $R_I = 35-70$ mm. Factor x_2 is a cylinder (left separating rod in dropper mechanism) radius in II area that ranged within following limits $R_{II} = 5-15$ mm. Factor x_2 is a cylinder (heddle eye of heald frame) radius in III area that ranged within following limits $R_{III} = 0.5-1.5$ mm.

Factor x_3 is a nominal value of the contact angle between cylinder (back rest) and yarns in I area that ranged within following limits $\varphi_{PI} = 75-125^\circ$. Factor x_3 is a nominal value of the contact angle between cylinder (left separating rod in the dropper mechanism) and yarns in II area that ranged within following limits $\varphi_{PII} = 25-75^\circ$. Factor x_3 is a nominal value of the contact angle between cylinder (heddle eye of heald frame) and yarns in III area ranged within following limits $\varphi_{PIII} = 14-20^\circ$.

At the first stage, tension in I area after back rest before separating cylindrical rod is determined. Table 2 represents orthogonal matrix for determining polyamide and basalt multifilament yarns tension in I area (variants 1-4).

Table 2 Orthogonal matrix for determining polyamide and basalt multifilament yarns tension in I area

№	Factors								
	x_1	Input tension [cN]				x_2	R_I [mm]	x_3	φ_{PI} [°]
		Variants 1-4							
		P_{0I1}	P_{0I2}	P_{0I3}	P_{0I4}				
1	+1	35	54	30	40	+1	70	+1	120
2	-1	27	42	22	30	+1	70	+1	120
3	+1	35	54	30	40	-1	40	+1	120
4	-1	27	42	22	30	-1	40	+1	120
5	+1	35	54	30	40	+1	70	-1	80
6	-1	27	42	22	30	+1	70	-1	80
7	+1	35	54	30	40	-1	40	-1	80
8	-1	27	42	22	30	-1	40	-1	80
9	-1.215	26	41	21	29	0	55	0	100
10	+1.215	36	55	31	41	0	55	0	100
11	0	31	48	26	35	-1.215	37	0	100
12	0	31	48	26	35	+1.215	73	0	100
13	0	31	48	26	35	0	55	-1.215	76
14	0	31	48	26	35	0	55	+1.215	124
15	0	31	48	26	35	0	55	0	100

Connection between denominated and coded values for I area is as follows:

variant 1

$$x_1 = \frac{P_{0I1} - 31}{4}, x_2 = \frac{R_I - 55}{15}, x_3 = \frac{\varphi_{PI} - 100}{20} \quad (2)$$

variant 2

$$x_1 = \frac{P_{0I2} - 48}{6}, x_2 = \frac{R_I - 55}{15}, x_3 = \frac{\varphi_{PI} - 100}{20} \quad (3)$$

variant 3

$$x_1 = \frac{P_{0I3} - 26}{4}, x_2 = \frac{R_I - 55}{15}, x_3 = \frac{\varphi_{PI} - 100}{20} \quad (4)$$

variant 4

$$x_1 = \frac{P_{0I4} - 35}{5}, x_2 = \frac{R_I - 55}{15}, x_3 = \frac{\varphi_{PI} - 100}{20} \quad (5)$$

At the second stage, tension in II area after cylindrical separating rod before shedding

mechanism on the loom. As input tension $P_{0II1} \div P_{0II4}$, output tension of warp yarns after II area is taken. Table 3 represents orthogonal matrix used to determine polyamide and basalt multifilament yarns tension in II area (variants 1-4).

Table 3 Orthogonal matrix for determining polyamide and basalt multifilament yarns tension in II area

№	Factors								
	x_1	Input tension [cN]				x_2	R_{II} [mm]	x_3	φ_{PII} [°]
		Variants 1-4							
		P_{0II1}	P_{0II2}	P_{0II3}	P_{0II4}				
1	+1	68	90	35	47	+1	14	+1	70
2	-1	40	50	27	37	+1	14	+1	70
3	+1	68	90	35	47	-1	6	+1	70
4	-1	40	50	27	37	-1	6	+1	70
5	+1	68	90	35	47	+1	14	-1	30
6	-1	40	50	27	37	+1	14	-1	30
7	+1	68	90	35	47	-1	6	-1	30
8	-1	40	50	27	37	-1	6	-1	30
9	-1.215	37	46	26	36	0	10	0	50
10	+1.215	71	94	36	48	0	10	0	50
11	0	54	70	31	42	-1.215	5	0	50
12	0	54	70	31	42	+1.215	15	0	50
13	0	54	70	31	42	0	10	-1.215	26
14	0	54	70	31	42	0	10	+1.215	74
15	0	54	70	31	42	0	10	0	50

Connection between denominated and coded values for II area is as follows:

variant 1

$$x_1 = \frac{P_{0II1} - 54}{14}, x_2 = \frac{R_{II} - 10}{4}, x_3 = \frac{\varphi_{PII} - 50}{20} \quad (6)$$

variant 2

$$x_1 = \frac{P_{0II2} - 70}{20}, x_2 = \frac{R_{II} - 10}{4}, x_3 = \frac{\varphi_{PII} - 50}{20} \quad (7)$$

variant 3

$$x_1 = \frac{P_{0II3} - 31}{4}, x_2 = \frac{R_{II} - 10}{4}, x_3 = \frac{\varphi_{PII} - 50}{20} \quad (8)$$

variant 4

$$x_1 = \frac{P_{0II4} - 42}{5}, x_2 = \frac{R_{II} - 10}{4}, x_3 = \frac{\varphi_{PII} - 50}{20} \quad (9)$$

At the third stage, tension in III area after shedding mechanism before weaving area of polyamide and basalt industrial fabrics. As input tension $P_{0III1} \div P_{0III4}$, output tension of warp yarns after III area is taken. Table 4 represents orthogonal matrix used to determine polyamide and basalt multifilament yarns tension in III area (variants 1-4).

Connection between denominated and coded values for III area is as follows:

variant 1

$$x_1 = \frac{P_{0III1} - 65}{20}, x_2 = \frac{R_{III} - 1}{0.4}, x_3 = \frac{\varphi_{PIII} - 20}{5} \quad (10)$$

variant 2

$$x_1 = \frac{P_{0III2} - 85}{25}, x_2 = \frac{R_{III} - 1}{0.4}, x_3 = \frac{\varphi_{PIII} - 20}{5} \quad (11)$$

variant 3

$$x_1 = \frac{P_{0III3} - 35}{6}, x_2 = \frac{R_{III} - 1}{0.4}, x_3 = \frac{\varphi_{PIII} - 20}{5} \quad (12)$$

variant 4

$$x_1 = \frac{P_{0III4} - 47}{7}, x_2 = \frac{R_{III} - 1}{0.4}, x_3 = \frac{\varphi_{PIII} - 20}{5} \quad (13)$$

Table 4 Orthogonal matrix for determining polyamide and basalt multifilament yarns tension in III area

№	Factors								
	Input tension [cN]					Curvature radius		Contact angle	
	x_1	Variants 1-4				x_2	R_{III} [mm]	x_3	φ_{PIII} [°]
P_{0III1}		P_{0III2}	P_{0III3}	P_{0III4}					
1	+1	85	110	41	54	+1	1.4	+1	25
2	-1	45	60	29	40	+1	1.4	+1	25
3	+1	85	110	41	54	-1	0.6	+1	25
4	-1	45	60	29	40	-1	0.6	+1	25
5	+1	85	110	41	54	+1	1.4	-1	15
6	-1	45	60	29	40	+1	1.4	-1	15
7	+1	85	110	41	54	-1	0.6	-1	15
8	-1	45	60	29	40	-1	0.6	-1	15
9	-1.215	41	55	28	38	0	1	0	20
10	+1.215	89	115	42	56	0	1	0	20
11	0	65	85	35	47	-1.215	0.5	0	20
12	0	65	85	35	47	+1.215	1.5	0	20
13	0	65	85	35	47	0	1	-1.215	14
14	0	65	85	35	47	0	1	+1.215	21
15	0	65	85	35	47	0	1	0	20

Experimental researches were conducted using a specific strain-gauge unit. Its design is described in details in papers [8-12]. Its peculiar feature is that a simulator of condition of interaction between guides and operative parts of looms comprised a set of cylindrical rods, a backrest, a separating rode of dropper mechanism, and heddles of heald frames of looms, with commensurable diameters.

3 RESULTS AND DISCUSSION

Resulting from implemented plan of the experiment (Table 2) for variant 1 (A), variant 2 (B), variant 3 (C) and variant 4 (D), I area, there were 10 parallel measurements for each variant. Table 5 represents average values of polyamide and basalt multifilament yarns tension for I area.

Known method for determination of coefficients in the regression equation (1) for second-order orthogonal matrix [9-11] was applied taking into account dependencies (2-5), and therefore regression dependencies were obtained for I area:

variant 1A

$$P_{I1} = 3.29 + 0.0008P_{0I1}R_I - 0.001P_{0I1}^2 + 0.0041P_{0I1}\varphi_{PI} + 0.95P_{0I1} - 0.000076R_I^2 + 0.00042R_I\varphi_{PI} - 0.032R_I + 0.00018\varphi_{PI}^2 - 0.044\varphi_{PI}, \quad (14)$$

variant 2B

$$P_{I2} = 5.66 + 0.00056P_{0I2}R_I - 0.0001P_{0I2}^2 + 0.0038P_{0I2}\varphi_{PI} + 0.89P_{0I2} - 0.00028R_I^2 + 0.0005R_I\varphi_{PI} - 0.0067R_I + 0.00029\varphi_{PI}^2 - 0.062\varphi_{PI}, \quad (15)$$

variant 3C

$$P_{I3} = 1.57 + 0.00021P_{0I3}R_I + 0.00001P_{0I3}^2 + 0.0033P_{0I3}\varphi_{PI} + 0.94P_{0I3} + 0.000004R_I^2 + 0.000042R_I\varphi_{PI} - 0.0064R_I + 0.000078\varphi_{PI}^2 - 0.017\varphi_{PI}, \quad (16)$$

variant 4D

$$P_{I4} = 2.33 + 0.0004P_{0I4}^2 + 0.0032P_{0I4}\varphi_{PI} + 0.91P_{0I4} + 0.00005R_I^2 - 0.0021R_I + 0.0001\varphi_{PI}^2 - 0.018\varphi_{PI}. \quad (17)$$

Adequacy of obtained regression dependencies were verified through SPSS program for statistical processing of experimental data [8, 10, 12].

Table 5 Results of series of experimental researches for I area aimed at determining combined influence of yarn tension before a guide, guide's surface radius and nominal value of contact angle to polyamide and basalt multifilament yarns tension after a guide for variant 1A, variant 2B, variant 3C and variant 4D

№	Factors			P_{I1}	P_{I2}	P_{I3}	P_{I4}
	x_1	x_2	x_3				
1	+1	+1	+1	52.5	79.4	41.1	54.7
2	-1	+1	+1	41.0	62.5	30.2	41.1
3	+1	-1	+1	51.3	77.8	40.9	54.6
4	-1	-1	+1	40.0	61.1	30.1	41.0
5	+1	+1	-1	45.9	69.9	37.0	49.3
6	-1	+1	-1	35.7	54.8	27.2	37.0
7	+1	-1	-1	45.2	68.9	36.9	49.2
8	-1	-1	-1	35.2	54.0	27.1	36.9
9	-1.215	0	0	36.6	56.7	27.3	37.7
10	+1.215	0	0	50.0	75.3	40.2	53.2
11	0	-1.215	0	42.8	65.2	33.7	45.4
12	0	+1.215	0	43.8	66.6	33.8	45.5
13	0	0	-1.215	40.0	61.2	31.7	42.7
14	0	0	+1.215	46.9	71.2	35.9	48.3
15	0	0	0	43.3	66.0	33.8	45.4

Resulting from implemented plan of the experiment (Table 3) for variant 1A, variant 2B, variant 3C and variant 4D for II area, there were 10 parallel measurements for each variant. Table 6 represents average values of polyamide and basalt multifilament yarns tension for II area.

Table 6 Results of series of experimental researches for II area aimed at determining combined influence of yarn tension before a guide, a guide's surface radius and a nominal value of contact angle to a polyamide and basalt multifilament yarns tension after a guide for variant 1A, variant 2B, variant 3C and variant 4D

№	Factors			P_{II1}	P_{II2}	P_{II3}	P_{II4}
	x_1	x_2	x_3				
1	+1	+1	+1	82.5	108.9	41.9	56.5
2	-1	+1	+1	49.1	61.2	32.3	44.5
3	+1	-1	+1	82.5	109.4	42.2	57.3
4	-1	-1	+1	49.1	61.4	32.5	45.1
5	+1	+1	-1	74.4	98.4	37.9	51.1
6	-1	+1	-1	43.9	54.9	29.3	40.2
7	+1	-1	-1	74.9	99.5	38.2	51.8
8	-1	-1	-1	44.3	55.5	29.4	40.7
9	-1.215	0	0	43.0	53.4	29.7	41.3
10	+1.215	0	0	81.8	108.2	41.1	55.1
11	0	-1.215	0	62.9	81.7	35.6	48.9
12	0	+1.215	0	62.5	80.8	35.3	48.0
13	0	0	-1.215	58.7	76.1	33.3	45.4
14	0	0	+1.215	66.4	85.9	37.6	51.2
15	0	0	0	62.4	80.9	35.4	48.2

Considering dependencies (1, 6-9), the following regression dependencies for II area were obtained:

variant 1A

$$P_{II1} = 2.38 + 0.0025P_{0II1}\varphi_{P_{II}} - 0.00022P_{0II1}R_{II} - 0.00018P_{0II1}^2 + 1.02P_{0II1} + 0.009R_{II}^2 + 0.0005R_{II}\varphi_{P_{II}} - 0.27R_{II} + 0.00013\varphi_{P_{II}}^2 - 0.007\varphi_{P_{II}}, \quad (18)$$

variant 2B

$$P_{II2} = 3.41 + 0.0025P_{0II2}\varphi_{P_{II}} - 0.0013P_{0II2}R_{II} - 0.00011P_{0II2}^2 + 1.02P_{0II2} + 0.014R_{II}^2 + 0.0015R_{II}\varphi_{P_{II}} - 0.35R_{II} + 0.00019\varphi_{P_{II}}^2 - 0.014\varphi_{P_{II}} \quad (19)$$

variant 3C

$$P_{II3} = 0.39 + 0.0029P_{0II3}\varphi_{P_{II}} - 0.0024P_{0II3}R_{II} + 0.000056P_{0II3}^2 + 1.01P_{0II3} + 0.002R_{II}^2 - 0.00016R_{II}\varphi_{P_{II}} + 0.014R_{II} + 0.00007\varphi_{P_{II}}^2 - 0.012\varphi_{P_{II}}, \quad (20)$$

variant 4D

$$P_{II4} = 4.43 + 0.0034P_{0II4}\varphi_{P_{II}} - 0.0031P_{0II4}R_{II} - 0.0003P_{0II4}^2 + 1.29P_{0II4} + 0.009R_{II}^2 - 0.00031R_{II}\varphi_{P_{II}} - 0.15R_{II} + 0.00014\varphi_{P_{II}}^2 + 0.002\varphi_{P_{II}}. \quad (21)$$

Resulting from implemented plan of the experiment (Table 4) for variant 1A, variant 2B, variant 3C and variant 4D for III area, there were 10 parallel measurements for each variant. Table 7 represents average values of polyamide and basalt multifilament yarns tension for III area.

Considering dependencies (1, 10-13), the following regression dependencies for III area were obtained:

variant 1A

$$P_{III1} = 15.96 + 0.0028P_{0III1}\varphi_{P_{III}} - 0.27P_{0III1}R_{III} - 0.0005P_{0III1}^2 + 1.50P_{0III1} + 24.61R_{III}^2 - 0.063R_{III}\varphi_{P_{III}} - 49.13R_{III} - 0.016\varphi_{P_{III}}^2 + 0.70\varphi_{P_{III}}, \quad (22)$$

variant 2B

$$P_{III2} = 20.03 + 0.0032P_{0III2}\varphi_{P_{III}} - 0.45P_{0III2}R_{III} - 0.0013P_{0III2}^2 + 1.93P_{0III2} + 53.44R_{III}^2 - 0.1R_{III}\varphi_{P_{III}} - 103.95R_{III} - 0.045\varphi_{P_{III}}^2 + 1.87\varphi_{P_{III}}, \quad (23)$$

variant 3C

$$P_{III3} = 1.81 + 0.003P_{0III3}\varphi_{P_{III}} - 0.26P_{0III3}R_{III} + 0.0014P_{0III3}^2 + 1.32P_{0III3} + 7.44R_{III}^2 - 0.03R_{III}\varphi_{P_{III}} - 11.04R_{III} - 0.004\varphi_{P_{III}}^2 + 0.18\varphi_{P_{III}}, \quad (24)$$

variant 4D

$$P_{III4} = 1.89 + 0.0043P_{0III4}\varphi_{P_{III}} - 0.5P_{0III4}R_{III} - 0.0012P_{0III4}^2 + 1.92P_{0III4} + 22.81R_{III}^2 - 0.075R_{III}\varphi_{P_{III}} - 38.05R_{III} - 0.013\varphi_{P_{III}}^2 + 0.56\varphi_{P_{III}}. \quad (25)$$

Table 7 Results of series of experimental researches for III area aimed at determining combined influence of yarn tension before a guide, a guide's surface radius and a nominal value of contact angle to a polyamide and basalt multifilament yarns tension after a guide for variant 1A, variant 2B, variant 3C and variant 4D

№	Factors			P_{III1}	P_{III2}	P_{III3}	P_{III4}
	x_1	x_2	x_3				
1	+1	+1	+1	99.7	132.7	46.8	64.9
2	-1	+1	+1	53.0	72.3	32.7	47.6
3	+1	-1	+1	118.6	169.5	52.9	81.3
4	-1	-1	+1	63.1	90.9	36.3	58.3
5	+1	+1	-1	97.5	129.7	45.6	63.1
6	-1	+1	-1	51.8	70.6	31.9	46.3
7	+1	-1	-1	115.8	165.4	51.5	78.8
8	-1	-1	-1	61.5	88.7	35.2	56.5
9	-1.215	0	0	50.1	69.5	32.0	47.0
10	+1.215	0	0	108.1	146.0	49.0	70.6
11	0	-1.215	0	96.9	146.2	45.8	75.0
12	0	+1.215	0	75.0	100.4	39.0	54.9
13	0	0	-1.215	78.1	106.4	39.9	57.8
14	0	0	+1.215	79.4	108.1	40.6	58.9
15	0	0	0	79.2	107.9	40.5	58.8

Table 8 shows values of coefficients in regression equation (1) for variant 1A, variant 2B, variant 3C, and variant 4D for areas I-III.

Table 8 Values of coefficients in regression equation (1) for variant 1A, variant 2B, variant 3C, and variant 4D for areas I-III

Area	Variant 1A	Variant 2B	Variant 3C	Variant 4D
I	$b_0=43.3164$	$b_0=66.0042$	$b_0=33.7705$	$b_0=45.4185$
	$b_1=10.6505$	$b_1=15.4753$	$b_1=10.2362$	$b_1=12.684$
	$b_2=0.828585$	$b_2=1.16709$	$b_2=0.111143$	$b_2=0.093465$
	$b_3=5.60057$	$b_3=8.14443$	$b_3=3.44824$	$b_3=4.63301$
	$b_{11}=-0.03459$	$b_{11}=-0.00883$	$b_{11}=0.0018305$	$b_{11}=0.0213389$
	$b_{12}=0.1$	$b_{12}=0.1$	$b_{12}=0.025$	$b_{12}=0.005$
	$b_{13}=0.65$	$b_{13}=0.9$	$b_{13}=0.525$	$b_{13}=0.65$
	$b_{22}=-0.03459$	$b_{22}=-0.12954$	$b_{22}=0.0018305$	$b_{22}=0.0213389$
	$b_{23}=0.25$	$b_{23}=0.3$	$b_{23}=0.025$	$b_{23}=0.003$
	$b_{33}=0.146469$	$b_{33}=0.232582$	$b_{33}=0.062185$	$b_{33}=0.0816941$
II	$b_0=62.4341$	$b_0=80.8843$	$b_0=35.3991$	$b_0=48.2046$
	$b_1=31.4385$	$b_1=44.8549$	$b_1=9.08171$	$b_1=11.3072$
	$b_2=-0.250117$	$b_2=-0.629054$	$b_2=-0.22736$	$b_2=-0.66441$
	$b_3=6.29525$	$b_3=7.99286$	$b_3=3.47099$	$b_3=4.78458$
	$b_{11}=-0.071782$	$b_{11}=-0.087629$	$b_{11}=0.0018307$	$b_{11}=-0.009596$
	$b_{12}=-0.025$	$b_{12}=-0.2$	$b_{12}=-0.075$	$b_{12}=-0.1$
	$b_{13}=1.425$	$b_{13}=2.05$	$b_{13}=0.475$	$b_{13}=0.55$
	$b_{22}=0.290349$	$b_{22}=0.455567$	$b_{22}=0.0621859$	$b_{22}=0.292179$
	$b_{23}=0.225$	$b_{23}=0.25$	$b_{23}=-0.025$	$b_{23}=-0.05$
	$b_{33}=0.109283$	$b_{33}=0.153791$	$b_{33}=0.0621859$	$b_{33}=0.111114$
III	$b_0=79.3285$	$b_0=108.604$	$b_0=40.4527$	$b_0=58.8568$
	$b_1=48.9418$	$b_1=65.9854$	$b_1=14.5986$	$b_1=19.4061$
	$b_2=-15.0595$	$b_2=-29.7256$	$b_2=-4.88838$	$b_2=-13.9428$
	$b_3=1.67467$	$b_3=2.33137$	$b_3=0.954776$	$b_3=1.55845$
	$b_{11}=-0.391306$	$b_{11}=-1.66357$	$b_{11}=0.0995578$	$b_{11}=-0.11970$
	$b_{12}=-4.35$	$b_{12}=-8.95$	$b_{12}=-1.275$	$b_{12}=-2.8$
	$b_{13}=0.55$	$b_{13}=0.8$	$b_{13}=0.175$	$b_{13}=0.3$
	$b_{22}=7.87736$	$b_{22}=17.1069$	$b_{22}=2.39306$	$b_{22}=7.30398$
	$b_{23}=-0.25$	$b_{23}=-0.4$	$b_{23}=-0.125$	$b_{23}=-0.3$
	$b_{33}=-0.813792$	$b_{33}=-2.26712$	$b_{33}=-0.202218$	$b_{33}=-0.662904$

Nominal contact angle between the guide and the yarns was taken as fixed value to determine combined influence of a polyamide and basalt multifilament yarns tension before the guide, a guide's surface radius, to a tension after the guide for I area in the system of equations (14-17).

The indicated value corresponded to the center of the experiment (Table 2). To get the nominal value of the contact angle in the center of the experiment $\varphi_{PI} = 100^\circ$ the following system of equations were obtained for I area:

variant 1A

$$P_{I1} = 0.67 + 1.35P_{0I1} + 0.009R_I - 0.0011P_{0I1}^2 - 0.0000R_I^2 + 0.00083P_{0I1}R_I, \quad (26)$$

variant 2B

$$P_{I2} = 2.36 + 1.27P_{0I2} + 0.043R_I - 0.00012P_{0I2}^2 - 0.00028R_I^2 + 0.00056P_{0I2}R_I, \quad (27)$$

variant 3C

$$P_{I3} = 0.64 + 1.26P_{0I3} - 0.002R_I + 0.000056P_{0I3}^2 + 0.0000028R_I^2 + 0.00021P_{0I3}R_I, \quad (28)$$

variant 4D

$$P_{I4} = 1.53 + 1.24P_{0I4} - 0.0021R_I + 0.00042P_{0I4}^2 + 0.000047R_I^2. \quad (29)$$

Figure 3 represents graphical dependencies depicting combined influence of polyamide and basalt multifilament yarns tension before the guide, guide's surface radius to the tension after the guide for I area, obtained with the help of equations (26-29), where the value of the nominal contact angle in the center of experiment was fixed $\varphi_{PI} = 100^\circ$.

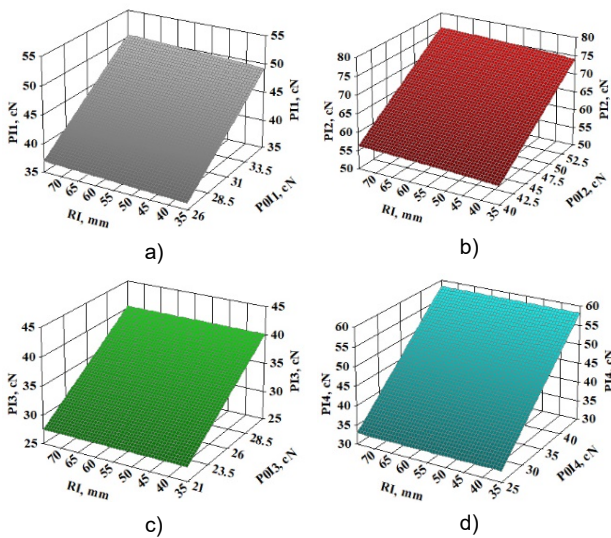


Figure 3 Graphical dependencies depicting combined influence of polyamide and basalt multifilament yarns tension before the guide, guide's surface radius to the tension after the guide for I area: a) polyamide multifilament yarn 174 tex; b) polyamide multifilament yarn 280.5 tex; c) basalt multifilament yarn 250 tex; d) basalt multifilament yarn 330 tex

Nominal contact angle between the guide and the yarns was taken as fixed value to determine combined influence of a polyamide and basalt multifilament yarns tension before the guide, a guide's surface radius, to a tension after the guide

for II area in the system of equations (18-21). The indicated value corresponded to the center of the experiment (Table 3). To get the nominal value of the contact angle in the center of the experiment $\varphi_{PII} = 50^\circ$ the following system of equations were obtained for II area:

variant 1A

$$P_{II1} = 2.35 + 1.15P_{0II1} - 0.20R_{II} - 0.00018P_{0II1}^2 + 0.009R_{II}^2 - 0.00022P_{0II1}R_{II}, \quad (30)$$

variant 2B

$$P_{II2} = 3.16 + 1.14P_{0II2} - 0.28R_{II} - 0.00011P_{0II2}^2 + 0.014R_{II}^2 - 0.0013P_{0II2}R_{II}, \quad (31)$$

variant 3C

$$P_{II3} = -0.015 + 1.15P_{0II3} - 0.0062R_{II} + 0.000056P_{0II3}^2 + 0.0019R_{II}^2 - 0.0024P_{0II3}R_{II}, \quad (32)$$

variant 4D

$$P_{II4} = 4.87 + 1.46P_{0II4} - 0.17R_{II} - 0.0003P_{0II4}^2 + 0.009R_{II}^2 - 0.0031P_{0II4}R_{II}. \quad (33)$$

Figure 4 represents graphical dependencies depicting combined influence of polyamide and basalt multifilament yarns tension before the guide, guide's surface radius to the tension after the guide for II area, obtained with the help of equations (30-33), where the value of the nominal contact angle in the center of experiment was fixed $\varphi_{PII} = 50^\circ$.

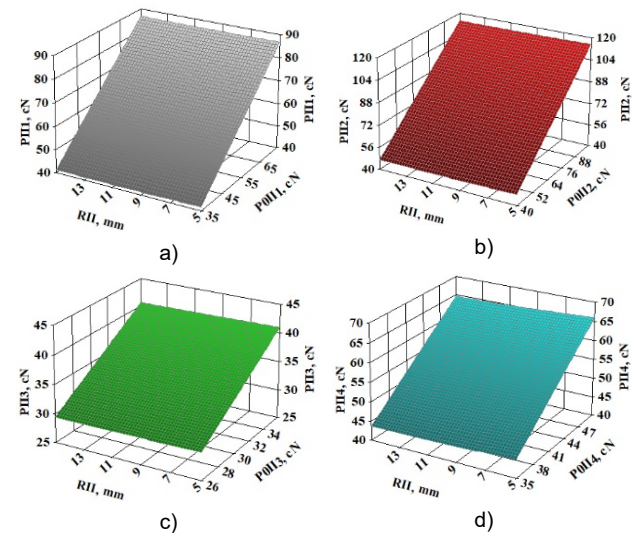


Figure 4 Graphical dependencies depicting combined influence of polyamide and basalt multifilament yarns tension before the guide, guide's surface radius to the tension after the guide for II area: a) polyamide multifilament yarn 174 tex; b) polyamide multifilament yarn 280.5 tex; c) basalt multifilament yarn 250 tex; d) basalt multifilament yarn 330 tex

Nominal contact angle between the guide and the yarns was taken as fixed value to determine

combined influence of a polyamide and basalt multifilament yarns tension before the guide, a guide's surface radius, to a tension after the guide for III area in the system of equations (22-25). The indicated value corresponded to the center of the experiment (Table 4). To get the nominal value of the contact angle in the center of the experiment $\varphi_{PIII} = 20^\circ$ the following system of equations were obtained for III area:

variant 1A

$$P_{III1} = 23.49 + 1.56P_{0III1} - 50.38R_{III} - 0.0005P_{0III1}^2 + 24.61R_{III}^2 - 0.27P_{0III1}R_{III}, \quad (34)$$

variant 2B

$$P_{III2} = 39.35 + 1.99P_{0III2} - 105.95R_{III} - 0.0013P_{0III2}^2 + 53.44R_{III}^2 - 0.45P_{0III2}R_{III}, \quad (35)$$

variant 3C

$$P_{III3} = 3.83 + 1.38P_{0III3} - 11.64R_{III} + 0.0014P_{0III3}^2 + 7.44R_{III}^2 - 0.27P_{0III3}R_{III}, \quad (36)$$

variant 4D

$$P_{III4} = 7.75 + 2.0P_{0III4} - 39.55R_{III} - 0.0012P_{0III4}^2 + 22.81R_{III}^2 - 0.5P_{0III4}R_{III}. \quad (37)$$

Figure 5 represents graphical dependencies depicting combined influence of polyamide and basalt multifilament yarns tension before the guide, guide's surface radius to the tension after the guide for III area, obtained with the help of equations (34-37), where the value of the nominal contact angle in the center of experiment was fixed $\varphi_{PIII} = 20^\circ$.

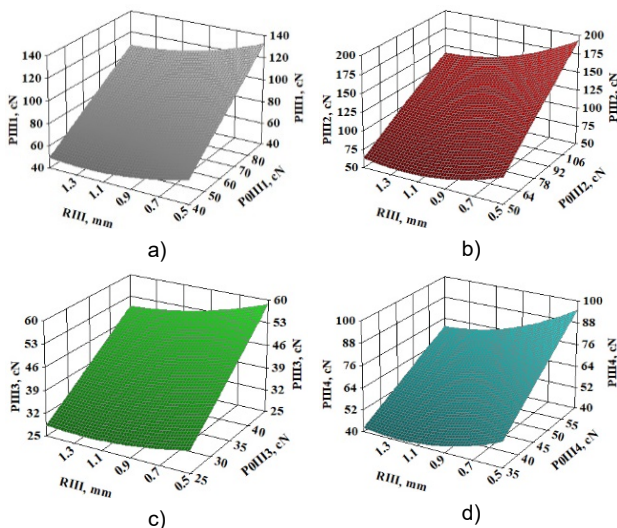


Figure 5 Graphical dependencies depicting combined influence of polyamide and basalt multifilament yarns tension before the guide, guide's surface radius to the tension after the guide for III area: a) polyamide multifilament yarn 174 tex; b) polyamide multifilament yarn 280.5 tex; c) basalt multifilament yarn 250 tex; d) basalt multifilament yarn 330 tex

In order to determine influence of guide's curve radius to polyamide and basalt multifilament yarn tension after the guide, for I area, in the system of equations (26-29) the value of tension before the guide was taken as fixed. This value corresponded to the center of experiment (Table 2). For polyamide multifilament yarn 174 tex, tension before the guide in the center of the experiment is $P_{0I1}=31$ cN. For polyamide multifilament yarn 280.5 tex, tension before the guide in the center of the experiment is $P_{0I2}=48$ cN. For basalt multifilament yarn 250 tex tension before the guide in the center of the experiment is $P_{0I3}=26$ cN. For basalt multifilament yarn 330 tex tension before the guide in the center of the experiment is $P_{0I4}=35$ cN. After inserting the indicated values, the following equations were obtained for I area:

variant 1A

$$P_{I1} = 41.49 + 0.035R_I - 0.000076R_I^2 \quad (38)$$

variant 2B

$$P_{I2} = 63.01 + 0.069R_I - 0.00028R_I^2 \quad (39)$$

variant 3C

$$P_{I3} = 33.58 + 0.0032R_I + 0.000004R_I^2 \quad (40)$$

variant 4D

$$P_{I4} = 45.39 - 0.0021R_I + 0.00005R_I^2 \quad (41)$$

Figure 6 represents graphical dependencies depicting influence of guide's curve radius to tension after the guide for I area, obtained with the help of equations (38-41), where the value of the polyamide and basalt multifilament yarns tension before the guide was fixed.

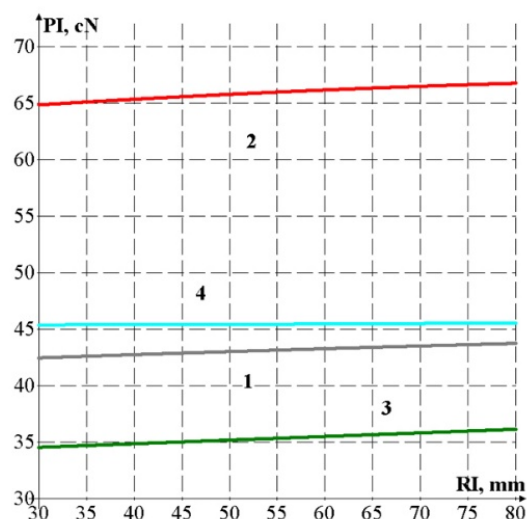


Figure 6 Graphical dependencies depicting influence of guide's curve radius to tension after the guide for I area: 1) polyamide multifilament yarn 174 tex; 2) polyamide multifilament yarn 280.5 tex; 3) basalt multifilament yarn 250 tex; 4) basalt multifilament yarn 330 tex

In order to determine influence of guide's curve radius to polyamide and basalt multifilament yarn tension after the guide, for II area, in the system of equations (30-33) the value of tension before the guide was taken as fixed. This value corresponded to the center of experiment (Table 3). For polyamide multifilament yarn 174 tex, tension before the guide in the center of the experiment is $P_{0II1}=54$ cN. For polyamide multifilament yarn 280.5 tex, tension before the guide in the center of the experiment is $P_{0II2}=70$ cN. For basalt multifilament yarn 250 tex tension before the guide in the center of the experiment is $P_{0II3}=31$ cN. For basalt multifilament yarn 330 tex tension before the guide in the center of the experiment is $P_{0II4}=42$ cN. After inserting the indicated values, the following equations were obtained for II area:

variant 1A

$$P_{II1} = 63.62 - 0.21R_{II} + 0.009R_{II}^2 \quad (42)$$

variant 2B

$$P_{II2} = 82.85 - 0.37R_{II} + 0.014R_{II}^2 \quad (43)$$

variant 3C

$$P_{II3} = 35.74 - 0.067R_{II} + 0.0019R_{II}^2 \quad (44)$$

variant 4D

$$P_{II4} = 65.73 - 0.29R_{II} + 0.009R_{II}^2 \quad (45)$$

Figure 7 represents graphical dependencies depicting influence of guide's curve radius to tension after the guide for II area, obtained with the help of equations (42-45), where the value of the polyamide and basalt multifilament yarns tension before the guide was fixed.

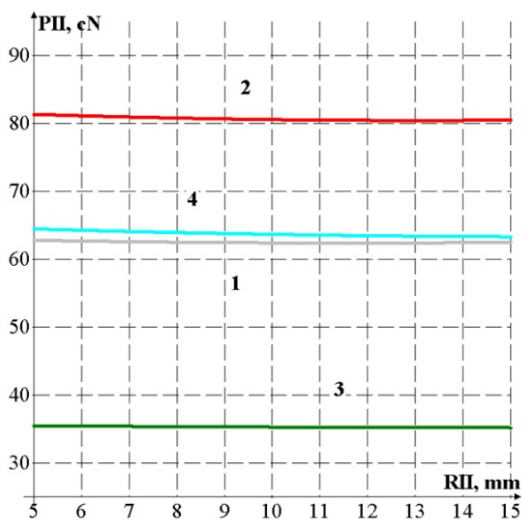


Figure 7 Graphical dependencies depicting influence of guide's curve radius to tension after the guide for II area: 1) polyamide multifilament yarn 174 tex; 2) polyamide multifilament yarn 280.5 tex; 3) basalt multifilament yarn 250 tex; 4) basalt multifilament yarn 330 tex

In order to determine influence of guide's curve radius to polyamide and basalt multifilament yarn tension after the guide, for III area, in the system of equations (34-37) the value of tension before the guide was taken as fixed. This value corresponded to the center of experiment (Table 4). For polyamide multifilament yarn 174 tex tension before the guide in the center of the experiment is $P_{0III1}=65$ cN. For polyamide multifilament yarn 280.5 tex tension before the guide in the center of the experiment is $P_{0III2}=85$ cN. For basalt multifilament yarn 250 tex tension before the guide in the center of the experiment is $P_{0III3}=35$ cN. For basalt multifilament yarn 330 tex tension before the guide in the center of the experiment is $P_{0III4}=47$ cN. After inserting the indicated values, the following equations were obtained for III area:

variant 1A

$$P_{III1} = 122.76 - 68.05R_{III} + 24.61R_{III}^2 \quad (46)$$

variant 2B

$$P_{III2} = 199.19 - 144.03R_{III} + 53.44R_{III}^2 \quad (47)$$

variant 3C

$$P_{III3} = 53.96 - 20.95R_{III} + 7.44R_{III}^2 \quad (48)$$

variant 4D

$$P_{III4} = 99.08 - 63.05R_{III} + 22.81R_{III}^2 \quad (49)$$

Figure 8 represents graphical dependencies depicting influence of guide's curve radius to tension after the guide for III area, obtained with the help of equations (46-49), where the value of the polyamide and basalt multifilament yarns tension before the guide was fixed.

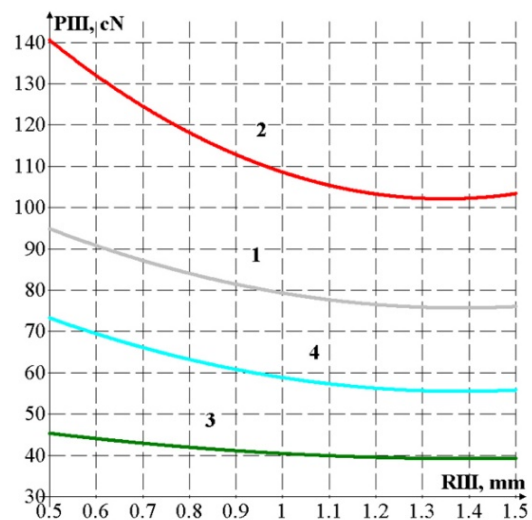


Figure 8 Graphical dependencies depicting influence of guide's curve radius to tension after the guide for III area: 1) polyamide multifilament yarn 174 tex; 2) polyamide multifilament yarn 280.5 tex; 3) basalt multifilament yarn 250 tex; 4) basalt multifilament yarn 330 tex

With the help of regression dependencies (22-25) the value of the warp yarns tension in the III area up to the fell of the multifilament and basalt fabrics were determined for different stages of weaving of the fabric element on the automatic looms. The value of warp yarns distortion at the stage of shedding, battening, and removal of fabric was taken into account as a value of the input tension in I area.

Having been analyzed, graphical dependencies (Figure 9) allowed to determine that the toughest conditions of weaving will be for variant 2B during manufacture of multilayer industrial fabric MTF-7; abovementioned is based on polyamide multifilament yarns 93.5x3 tex. This can be explained by the high value of the threading tension of warp yarns and coefficient of friction on the guide surfaces. When the diameter of warp polyamide multifilament yarns (variant 1A and variant 2B) and basalt multifilament yarns (variant 3C and variant 4D) density of weaving process increases, and such phenomena can be explained by tension in III area, which increases as a result of yarn diameter distortion in the contact area with guide and bending rigidity of yarns.

Obtained results can be applied to improve technological process of weaving, when density of weaving process can be determined yet during the initial stage.

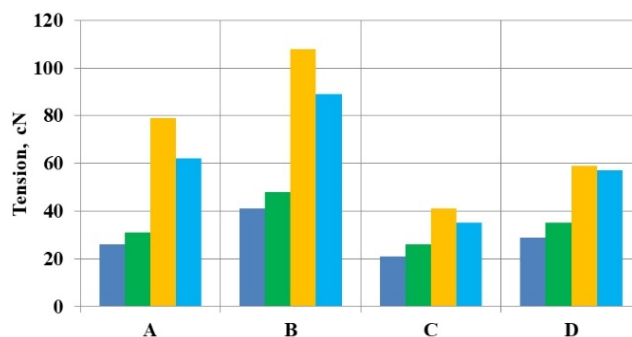


Figure 9 Histogram of warp yarns tension up to fell at the moment of fabric weaving in III area: A) multilayer industrial fabric MTF - 5 (warp – polyamide multifilament yarn 29x6 tex); B) multilayer industrial fabric MTF - 7 (warp – polyamide multifilament yarn 93.5x3 tex); C) basalt fabric of plain weave (warp – basalt multifilament yarn 250 tex); D) basalt fabric of plain weave (warp – basalt multifilament yarn 330 tex); ■ – threading tension of warp yarns; ■ – warp yarns tension working with closed shed; ■ – tension of warp yarns with fully opened shed; ■ – tension of warp yarns during battening

4 CONCLUSIONS

To enhance manufacturing processes of weaving production it is necessary to optimize manufacturing efforts based on maximum reduction of polyamide and basalt multifilament yarns tension in the industrial fabrics formation areas.

The researches performed to determine polyamide and basalt multifilament yarns tension when interacting with guides and operative parts of looms established increase in yarn tension according to filling areas. The above comes with change in geometrical dimensions of filling line and friction forces in the contact area.

The regression dependencies were obtained resulting from series of experimental researches performed to determine combined influence of polyamide and basalt multifilament yarns tension prior going to guide, guide's curve radius and nominal value of contact angle to yarn tension after the guide. Consistent use of regression dependencies data enables determining polyamide and basalt multifilament yarns tension before they enter industrial fabrics weaving area. The regression dependencies analysis has made it possible to establish manufacturing parameters, when polyamide and basalt multifilament yarns tension (before they enter industrial fabrics weaving area) will be of minimum value. As a result, it will be possible to minimize tension of polyamide and basalt multifilament yarns during their processing on looms. Mentioned results, when used, enable efficiency enhancement for polyamide and basalt multifilament yarns manufacturing process on production equipment as far as tension in the operational area of industrial fabrics weaving could be minimized, yarn breakages reduced and performance of textile and knitwear equipment improved.

Mentioned results can be used while enhancing efficiency of manufacturing process for single-layer and multilayer fabrics produced from multifilament yarns, which in terms of their physical and mechanical properties will be similar to polyamide and basalt multifilament yarns.

ACKNOWLEDGEMENT: We are really grateful to Danish Textiles management and Kyiv "Factory of Technical Fabrics TEKHNOFILTR" for raw materials provided for experimental work and possibility to try out results of our research in production environment.

5 REFERENCES

1. Koo Y., Kim H.: Friction of cotton yarn in relation to fluff formation on circular knitting machines, *Textile Research Journal* 72(1), 2002, pp.17-20, <https://doi.org/10.1177/004051750207200103>
2. Vasconcelos F.B., Marcicano J.P.P., Sanches R.A.: Influence of yarn tension variations before the positive feed on the characteristics of knitted fabrics, *Textile Research Journal* 85, 2015, pp.1864-1871, <https://doi.org/10.1177/0040517515576327>
3. Shcherban' V.Yu.: Determining the technological forces during beating-up in the production of multilayer industrial fabrics, *Technology of Textile Industry (Izvestiya Vysshikh Uchebnykh Zavedenii)* 3, 1990, pp.44-47 (in Russian)

4. Weber M.O., Ehrmann A.: Necessary modification of the Euler-Eytelwein formula for knitting machines, *The Journal of The Textile Institute* 103, 2012, pp. 687-690, <https://doi.org/10.1080/00405000.2011.598665>
5. Yakubitskaya I.A., Chugin V.V., Shcherban' V.Yu.: Dynamic analysis of the traversing conditions at the end sections of the groove in a winding drum, *Technology of Textile Industry (Izvestiya Vysshikh Uchebnykh Zavedenii)* 5, 1997, pp.33-36 (in Russian)
6. Yakubitskaya I.A., Chugin V.V., Shcherban' V.Yu.: Differential equations for relative yarn movement in the end sections of the channel in the winding drum, *Technology of Textile Industry (Izvestiya Vysshikh Uchebnykh Zavedenii)* 6, 1997, pp.50-54 (in Russian)
7. Shcherban' V.Yu.: Interaction of stiff yarns with the working parts of knitting and sewing machines, *Textile industry* 10, 1988, pp.53 (in Russian)
8. Shcherban' V., Melnyk G., Sholudko M., Kalashnyk V.: Warp yarn tension during fabric formation, *Vlakna a textil (Fibres and Textiles)* 25(2), 2018, pp.97-104, http://vat.ft.tul.cz/2018/2/VaT_2018_2_16.pdf
9. Shcherban' V., Melnyk G., Sholudko M., Kolysko O., Kalashnyk V.: Yarn tension while knitting textile fabric, *Vlakna a textil (Fibres and Textiles)* 25(3), 2018, pp.74-83, http://vat.ft.tul.cz/2018/3/VaT_2018_3_12.pdf
10. Shcherban' V., Kolysko O., Melnyk G., Sholudko M., Shcherban' Y. and Shchutska G.: Determining tension of yarns when interacting with guides and operative parts of textile machinery having the torus form, *Vlakna a textil (Fibres and Textiles)* 27(4), 2020, pp. 87-95, http://vat.ft.tul.cz/2020/4/VaT_2020_4_12.pdf
11. Shcherban' V., Makarenko J., Melnyk G., Shcherban' Y., Petko A., Kirichenko A.: Effect of the yarn structure on the tension degree when interacting with high-curved guides, *Vlakna a textil (Fibres and Textiles)* 26(4), 2019, pp.59-68, http://vat.ft.tul.cz/2019/4/VaT_2019_4_8.pdf
12. Shcherban' V., Makarenko J., Petko A., Melnyk G., Shcherban' Yu., Shchutska G.: Computer implementation of a recursion algorithm for determining the tension of a thread on technological equipment based on the derived mathematical dependencies, *Eastern-European Journal of Enterprise Technologies* 2/1, 2020, pp. 41-50, <https://doi.org/10.15587/1729-4061.2020.198286>
13. Shcherban' V., Melnyk G., Sholudko M., Kolysko O., Kalashnyk V.: Improvement of structure and technology of manufacture of multilayer technical fabric, *Vlakna a textil (Fibres and Textiles)* 26(2), 2019, pp.54-63, http://vat.ft.tul.cz/2019/2/VaT_2019_2_10.pdf
14. Kovar R.: Impact of directions on frictional properties of a knitted fabric, *Vlakna a textil (Fibres and Textiles)* 14(2), 2007, pp.15-20, http://vat.ft.tul.cz/Archive/VaT_2007_2.pdf
15. Donmez S., Marmarali A.: A Model for Predicting a Yarn's Knittability, *Textile Research Journal* 74, 2004, pp.1049-1054, <https://doi.org/10.1177/004051750407401204>
16. Liu X., Chen N., Feng X.: Effect of Yarn Parameters on the Knittability of Glass Ply Yarn, *Fibres & Textiles in Eastern Europe* 16, 2008, pp.90-93
17. Hammersley M.J.: 7-A Simple Yarn-friction Tester for use with knitting yarns, *The Journal of the Textile Institute* 64, 1973, pp.108-111, <https://doi.org/10.1080/00405007308630420>
18. Sodomka L., Chrpová E.: Method of determination of Euler friction coefficients of textiles, *Vlakna a textil (Fibres and Textiles)* 15(2-3), 2008, pp.28-33, http://vat.ft.tul.cz/Archive/VaT_2008_2_3.pdf
19. Vasilchenko V.N., Shcherban' V.Yu.: Effect of the twist of Kapron filament yarn on its bending rigidity, *Technology of Textile Industry (Izvestiya Vysshikh Uchebnykh Zavedenii)* 4, 1986, pp.8-9 (in Russian)
20. Vasilchenko V.N., Shcherban' V.Yu., Apokin Ts.V.: Attachment for holding multilayer fabrics in the clamps of a universal tensile tester, *Textile industry* 8, 1987, pp.62 (in Russian)
21. Shcherban' V., Korogod G., Chaban V., Kolysko O., Shcherban' Yu., Shchutska G.: Computer simulation methods of redundant measurements with the nonlinear transformation function, *Eastern-European Journal of Enterprise Technologies* 2/5, 2019, pp.16-22, <https://doi.org/10.15587/1729-4061.2019.160830>
22. Shcherban' V., Korogod G., Kolysko O., Kolysko M., Shcherban' Yu., Shchutska G.: Computer simulation of multiple measurements of logarithmic transformation function by two approaches, *Eastern-European Journal of Enterprise Technologies* 6/4, 2020, pp. 6-13, <https://doi.org/10.15587/1729-4061.2020.218517>